

## Supporting Information

# **Solid-Phase Synthesis of BODIPY Dyes and Development of an Immunoglobulin Fluorescent Sensor**

Marc Vendrell, Gaddamanugu Gopi Krishna, Krishna Kanta Ghosh, Duanting Zhai, Jun-  
Seok Lee, Qing Zhu, Yin Hoe Yau, Susana Geifman Shochat, Hyori Kim, Junho Chung,  
Young-Tae Chang

List of contents:

1. General procedures (synthesis, screening, SPR and Job plot analysis) and characterization for **1-3**.
2. Chemical structures and characterization data for the **BDM** library.
3. Characterization data for **Ig Orange (BDM-69)**.
4. Extended screening of **Ig Orange (BDM-69)**.
5. **Ig Orange** response against IgG in human serum samples.
6. Characterization of biotinylated human IgG.
7. Structure-fluorescence relationships of **Ig Orange** and additional SPR experiments.
8. Binding of **Ig Orange** to polyclonal IgG and monoclonal IgG<sub>1</sub>.
9. Fractional saturation curve experiments of **Ig Orange**.

## **1. General procedures (synthesis, screening, SPR and Job plot analysis) and characterization for 1-3.**

**Synthesis. General.** All the chemicals (building block aldehydes plus others) and solvents were purchased from Sigma Aldrich, Alfa Aesar, Fluka, MERCK or Acros, and used without further purification. 2-chlorotriyl chloride polystyrene resin (100-200 mesh, 1% DVB cross-linking) was purchased from BeadTech (Korea). Human immunoglobulins (G, A and M), immunoglobulin-depleted human serum and other reagents used for the biological characterization were supplied by Sigma Aldrich. Normal phase purifications were carried out using Merck Silica Gel 60 (particle size: 0.040-0.063 mm, 230-400 mesh). Analytical characterization was performed on a HPLC-MS (Agilent-1200 series) with a DAD detector and a single quadrupole mass spectrometer (6130 series) with an ESI probe. Analytical method, unless indicated: eluents: A: H<sub>2</sub>O (0.1% HCOOH), B: ACN (0.1% HCOOH), gradient from 5 to 95% B in 10 min; C<sub>18</sub>(2) Luna column (4.6 × 50 mm<sup>2</sup>, 5 μm particle size). <sup>1</sup>H-NMR, <sup>19</sup>F-NMR and <sup>13</sup>C-NMR spectra were recorded on Bruker Avance 300 NMR spectrometer, and chemical shifts are expressed in parts per million (ppm). For <sup>19</sup>F-NMR, trifluoroacetic acid was used as a reference (δ = 0.00 ppm). Spectroscopic and quantum yield data were measured on a SpectraMax M2 spectrophotometer (Molecular Devices), and the data analysis was performed using GraphPrism 5.0.

**(9H-fluoren-9-yl)methyl 3-oxo-3-(1H-pyrrol-2-yl)propylcarbamate (1).** Fmoc-β-Ala-OH (2.5 g, 8.0 mmol) was dissolved in dry THF. 2,2'-dipyridyl disulfide (2.7 g, 12.0 mmol) and PPh<sub>3</sub> (4.2 g, 16.0 mmol) were added, and the mixture was stirred under N<sub>2</sub> atmosphere at r.t for 24 h. In a separate flask, methylmagnesium bromide (12 mL of a 3.0

M solution in THF, 36.0 mmol) was added dropwise at  $-78\text{ }^{\circ}\text{C}$  to a solution of pyrrole (3.3 mL, 48.0 mmol) in dry THF (50 mL). The mixture was stirred at  $-78\text{ }^{\circ}\text{C}$  for 30 min and at  $-20\text{ }^{\circ}\text{C}$  for another 30 min. Then the thioester crude mixture (after 24 h reaction) was added drop wise at  $-78\text{ }^{\circ}\text{C}$ , and the whole solution was stirred at  $-78\text{ }^{\circ}\text{C}$  for 30 min and another 30 min at r.t. The reaction was quenched with a saturated solution of  $\text{NH}_4\text{Cl}$ . After dilution with diethyl ether, the organic layer was washed with water ( $3 \times 100\text{ mL}$ ) and brine (100 mL), dried over anhydrous sodium sulfate and evaporated under vacuum. Column chromatography (elution with hexane-ethyl acetate 1:1) rendered 2.53 g of **1** as a white solid (yield: 88%). ESI  $m/z$  ( $\text{C}_{22}\text{H}_{20}\text{N}_2\text{O}_3$ ), calc: 359.2; found ( $\text{M}+\text{Na}^+$ ): 382.9.  $^1\text{H}$ -NMR (300 MHz,  $\text{CDCl}_3$ ): 9.68 (bs, 1H), 7.75 (d, 2H,  $J = 7.3\text{ Hz}$ ), 7.57 (d, 2H,  $J = 7.8\text{ Hz}$ ), 7.38 (t, 2H,  $J = 7.6\text{ Hz}$ ), 7.28 (t, 2H,  $J = 7.3\text{ Hz}$ ), 7.04 (bs, 1H), 6.94 (bs, 1H), 6.28 (d, 1H,  $J = 2.9\text{ Hz}$ ), 5.48 (bt, 1H,  $J = 5.9\text{ Hz}$ ), 4.38 (d, 2H,  $J = 7.0\text{ Hz}$ ), 4.20 (t, 1H,  $J = 7.0\text{ Hz}$ ), 3.61 (dt, 2H,  $J = 5.9\text{ Hz}$ , 6.1 Hz), 3.06 (t, 2H,  $J = 5.9\text{ Hz}$ ).  $^{13}\text{C}$ -NMR (75 MHz,  $\text{CDCl}_3$ ): 189.0, 156.4, 143.9, 141.3, 131.7, 127.6, 127.0, 125.1, 124.9, 119.9, 116.8, 110.9, 66.7, 47.2, 37.6, 36.3.

**10-(2-(((9H-fluoren-9-yl)methoxy)carbonylamino)ethyl)-5,5-difluoro-1,3-dimethyl-5H-dipyrrolo[1,2-c:1',2'-f][1,3,2]diazaborinin-4-ium-5-uide (2).** **1** (1.5 g, 4.2 mmol) and 2,4-dimethylpyrrole (692  $\mu\text{L}$ , 6.7 mmol) were dissolved in  $\text{CH}_2\text{Cl}_2$  at  $0\text{ }^{\circ}\text{C}$ . After 10 min stirring, the mixture was treated drop wise with  $\text{POCl}_3$  (1.3 g, 8.4 mmol), and the resulting solution was stirred at  $0\text{ }^{\circ}\text{C}$  for 1 h, and at  $35\text{ }^{\circ}\text{C}$  for 20 h. Afterwards, DIEA (2.9 mL, 16.8 mmol) and  $\text{BF}_3\cdot\text{OEt}_2$  (2.3 mL, 16.8 mmol) were added and the crude mixture was stirred for 4 h at r.t. Column chromatography (elution with hexane-ethyl acetate 4:1) rendered 1.2 g of **2** as a reddish solid (yield: 57%). ESI  $m/z$  ( $\text{C}_{28}\text{H}_{26}\text{BF}_2\text{N}_3\text{O}_2$ ),

calc: 485.2; found (M-F): 466.3.  $^1\text{H-NMR}$  (300 MHz,  $\text{CDCl}_3$ ): 7.77 (d, 2H,  $J = 7.6\text{Hz}$ ), 7.61 (bs, 1H), 7.56 (d, 2H,  $J = 7.0\text{Hz}$ ), 7.41 (t, 2H,  $J = 7.6\text{Hz}$ ), 7.31 (t, 2H,  $J = 7.3\text{Hz}$ ), 7.11 (d, 1H,  $J = 3.5\text{Hz}$ ), 6.42 (d, 1H,  $J = 3.2\text{Hz}$ ), 6.17 (bs, 1H), 5.10 (bt, 1H,  $J = 6.2\text{Hz}$ ), 4.43 (d, 2H,  $J = 6.7\text{Hz}$ ), 4.19 (t, 1H,  $J = 6.7\text{Hz}$ ), 3.50 (dt, 2H,  $J = 6.7\text{ Hz}, 7.2\text{Hz}$ ), 3.18 (t, 2H,  $J = 7.0\text{Hz}$ ), 2.58 (s, 3H), 2.46 (s, 3H).  $^{13}\text{C-NMR}$  (75 MHz,  $\text{CDCl}_3$ ): 161.2, 156.3, 145.2, 145.1, 143.7, 142.3, 141.3, 138.2, 134.0, 127.7, 127.0, 125.0, 124.0, 123.8, 120.0, 116.1, 66.8, 47.2, 42.8, 30.1, 16.2, 15.0.  $^{19}\text{F-NMR}$  (282 MHz,  $\text{CDCl}_3$ ): -70.31, -70.53 (dd,  $J = 31\text{Hz}, J = 62\text{Hz}, \text{BF}_2$ ).<sup>1,2</sup>

**10-(2-aminoethyl)-5,5-difluoro-1,3-dimethyl-5H-dipyrrolo[1,2-c:1',2'-**

**f][1,3,2]diazaborinin-4-ium-5-uide hydrochloride (3).** A solution of **2** (1.0 g, 2.06 mmol) in  $\text{CH}_2\text{Cl}_2$  was treated with DBU every 15 min for a total of 4 times ( $4 \times 73 \mu\text{L}$ ,  $4 \times 0.51 \text{ mmol}$ ) and a total reaction time of 1 h. Afterwards, the reaction was quenched with a aqueous solution of 0.5 N HCl and stirred for 15 min at r.t. The resulting red solid was filtered off, and thoroughly washed with diethyl ether to render 350 mg of **3** as the hydrochloride salt (yield: 65%). ESI  $m/z$  ( $\text{C}_{13}\text{H}_{16}\text{BF}_2\text{N}_3$ ), calc: 263.1; found (M-F): 244.1.  $^1\text{H-NMR}$  (300 MHz,  $\text{DMSO-d}_6$ ): 8.51 (bs, 2H), 7.65 (s, 1H), 7.63 (s, 1H), 6.52 (s, 1H), 6.46 (s, 1H), 3.37 (m, 2H), 3.16 (s, 3H), 3.03 (m, 2H), 2.50 (s, 3H).  $^{13}\text{C-NMR}$  (75 MHz,  $\text{DMSO-d}_6$ ): 161.6, 146.3, 141.0, 138.0, 133.5, 133.3, 124.7, 124.0, 116.1, 48.5, 47.8, 15.9, 14.6.  $^{19}\text{F-NMR}$  (282 MHz,  $\text{DMSO-d}_6$ ): -66.97, -67.19 (dd,  $J = 29\text{Hz}, J = 61\text{Hz}, \text{BF}_2$ ).

**Synthesis of the BDM Library.** A solution of **3** (350 mg, 1.3 mmol) and DIEA (1.1 mL, 6.5 mmol) was dissolved in *N*-methylpyrrolidone (NMP) and added to 2-chlorotriptyl chloride polystyrene resin (loading: 1.2 mmol/g, 3.3 g, 3.9 mmol). The reaction was

shaken at r.t. for 16 h, after which the resin was capped with MeOH (0.8 mL/g resin) for 4 h, and finally filtered off and washed with NMP, DMF and DCM ( $\times 4$  each solvent). For every compound, 50 mg of the loaded resin (corresponding to 0.06 mmol of **3**) were re-suspended in 2 mL DMSO-ACN (1:1), and treated with pyrrolidine (75  $\mu$ L, 0.9 mmol), AcOH (54  $\mu$ L, 0.9 mmol) and the corresponding aldehydes (0.9 mmol). The resulting suspension was heated at 85  $^{\circ}$ C for 5 min, cooled down to r.t., filtered off, and washed with DMF and DCM ( $\times 4$  each solvent). Afterwards, the resins were treated with a solution of TFA-DCM (0.5:99.5) ( $2 \times 10$  min), and the resulting filtrates were combined and evaporated under pressure. **BDM** products were isolated as the free-amine compounds after silica-based SPE elution with DCM-MeOH (98:2) containing 1%  $\text{NH}_3_{\text{conc}}$  in MeOH (full characterization data on Table S1). **Ig Orange (BDM-69)**:  $^1\text{H-NMR}$  (300 MHz,  $\text{CDCl}_3$ ): 7.57-7.61-7.69 (m, 8H), 7.39 (d, 4H,  $J = 7.6\text{Hz}$ ), 7.17 (d, 4H,  $J = 8.8\text{Hz}$ ), 6.80 (s, 1H), 6.50 (dd, 1H,  $J = 2.1\text{Hz}$ ,  $J = 4.0\text{Hz}$ ), 3.18 (d, 2H,  $J = 6.4\text{Hz}$ ), 3.12 (d, 2H,  $J = 6.4\text{Hz}$ ), 2.54 (s, 3H), 1.63 (bs, 2H).  $^{13}\text{C-NMR}$  (75 MHz,  $\text{CDCl}_3$ ): 157.0, 143.9, 140.6, 139.2, 138.9, 137.8, 136.9, 135.0, 134.4, 129.8, 128.6, 128.2, 127.8, 127.8, 126.9, 126.5, 123.4, 122.1, 119.7, 118.0, 116.0, 77.2, 43.4, 31.8, 29.5, 16.2.  $^{19}\text{F-NMR}$  (282 MHz,  $\text{CDCl}_3$ ): -65.82, -66.03 (dd,  $J = 30\text{Hz}$ ,  $J = 59\text{Hz}$ ,  $\text{BF}_2$ ).

**Quantum Yield Measurements.** Quantum yields were calculated by measuring the integrated emission area of the fluorescent spectra, and referring them to the area measured for Rhodamine B in EtOH after excitation at 510 nm ( $\Phi_{\text{Rho-B}} = 0.70$ ). Quantum yields for the **BDM** products were then calculated using equation below, where  $F$  represents the area of fluorescent emission,  $n$  is reflective index of the solvent, and  $Abs$  is

absorbance at excitation wavelength selected for standards and samples. Emission was integrated from 540 nm to 800 nm.

$$\Phi_{flu}^{sample} = \Phi_{fl}^{reference} \left( \frac{F^{sample}}{F^{reference}} \right) \left( \frac{\eta^{sample}}{\eta^{reference}} \right) \left( \frac{Abs^{reference}}{Abs^{sample}} \right)$$

**Screening of the BDM Library.** Fluorescence intensities were measured using a Spectra Max Gemini XSF plate reader in a 384-well plate. **BDM** compounds were dissolved to a final concentration of 10  $\mu$ M (20 mM HEPES buffer, pH 7.4, containing 1% DMSO) and incubated with different proteins and peptides at different serial concentrations in 20 mM HEPES buffer (pH 7.4). The excitation wavelength was set at 510 nm, and the emission spectra were recorded from 560 to 700 nm. Fluorescence fold increase ratios were determined by referring the maximum fluorescence intensity emission of **BDM** compounds in the presence of the screened proteins and peptides to the maximum fluorescence intensity emission of **BDM** compounds in 20 mM HEPES buffer (pH 7.4).

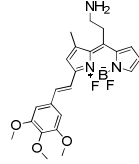
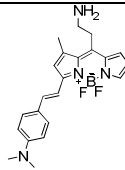
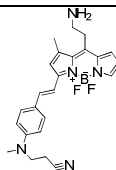
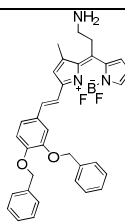
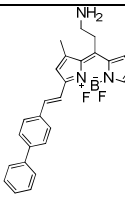
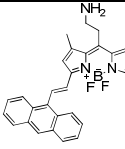
**Surface Plasmon Resonance.** Human IgG (5.0 mg, 0.033  $\mu$ mol) and biotin-OSu (0.11 mg, 0.33  $\mu$ mol) were dissolved in 0.1 M NaHCO<sub>3</sub> (pH 8.5) and shaken for 1 h at 25 °C. Excess of biotinylating reagent was removed by centrifugation with Microcon 30K filters (3 rounds at 14,000 rpm for 20 min at 4 °C). The purified biotinylated IgG was resuspended in PBS, and characterized by SDS-PAGE and Western blotting with HRP-conjugated streptavidin (Figure S6 in SI). The concentration of biotinylated IgG before fluorescence and SPR experiments was determined by Bradford assay. SPR measurements were performed on a T-200 instrument (Biacore AB, GE Healthcare) equipped with Series S sensor chip CM7 (Biacore AB, GE Healthcare). All experiments were performed at 25 °C as previously described.<sup>3</sup> Briefly, the carboxymethylated sensor surface was activated for 7 min with 1:1 of 0.2 M EDC (*N*-ethyl-*N'*-[3-(diethylamino)

propyl] carbodiimide) and 50 mM NHS (*N*-hydroxysuccinimide), then human IgG was coupled to 12,000 RU and finally the surface was deactivated for 7 min with 1 M ethanolamine-HCl (pH 8.5). The immobilized immunoglobulin was probed with one positive- and one negative-binding fragment diluted into the running buffer (10 mM sodium phosphate buffer, 150 mM NaCl, 1% DMSO, pH 7.4) to ascertain its functionality. **Ig Orange** (0.07, 0.21, 0.62, 1.86, 5.57 and 16.7  $\mu$ M, in duplicates) was injected across a control surface and the immobilized surface serially. Sensorgrams obtained were DMSO calibrated and buffer- and reference-subtracted.<sup>4</sup> Responses at equilibrium were plotted against analyte concentration and fit to a simple isotherm to obtain the affinity constant using Scrubber 2 software (BioLogics Inc. Australia).

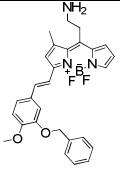
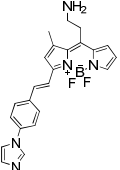
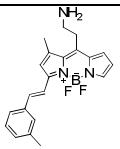
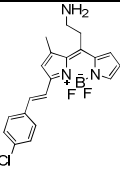
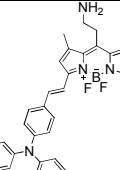
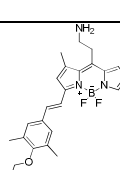
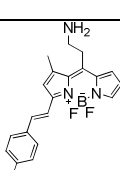
**Job Plot Analysis.** **Ig Orange** (final concentrations: 0, 1.6, 3.2, 4.8, 6.4, 8.0, 9.6, 11.2, 12.8, 14.4, 16  $\mu$ M) and human IgG (final concentrations: 16, 14.4, 12.8, 11.2, 9.6, 8.0, 6.4, 4.8, 3.2, 1.6, 0  $\mu$ M) were incubated in PBS buffer (pH 7.3) containing 1% DMSO, and the fluorescence intensities of the different solutions were recorded on a SpectraMax M2 plate reader (excitation: 530 nm; emission: 590 nm). The Job plot is represented as [fluorescence fold increase  $\times$  ratio **Ig Orange**] vs. ratio **Ig Orange**, with values as means ( $n=3$ ) and error bars as standard deviations.

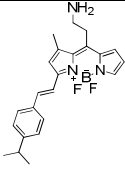
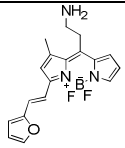
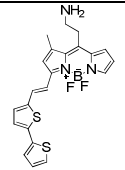
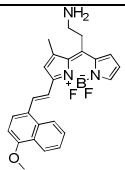
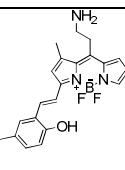
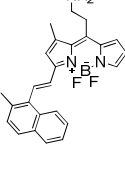
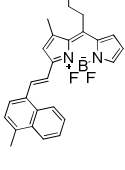
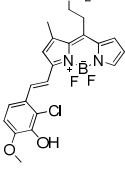
## 2. Chemical structures and characterization data for the BDM library.

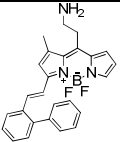
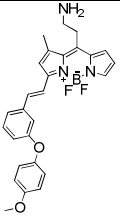
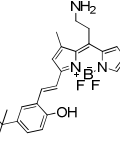
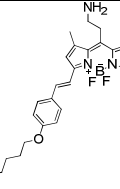
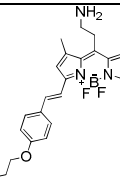
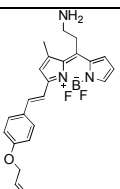
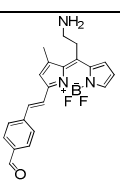
Table S1. Chemical structures and characterization data for the BDM library.

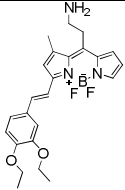
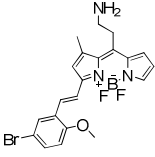
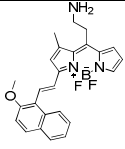
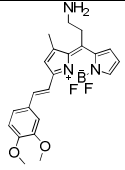
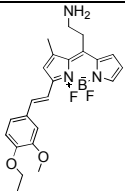
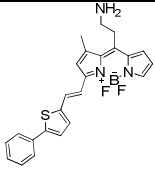
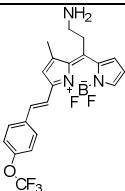
Code	Structure	Mcalc.	Mexp.	tR (min)	purity	$\lambda_{\max}$ (ABS)	$\lambda_{\max}$ (EM)	$\phi$	mg
BDM-1		441.3	422.0	3.74	87%	561	586	0.21	5.1
BDM-2		394.3	375.0	3.96	88%	607	685	0.01	5.8
BDM-3		433.3	414.0	4.02	87%	600	683	0.05	5.9
BDM-4		563.4	543.9	5.48	95%	566	590	0.42	6.1
BDM-5		427.3	408.0	5.16	96%	561	575	0.50	7.7
BDM-6		451.3	432.0	4.97	89%	536	682	0.12	9.0



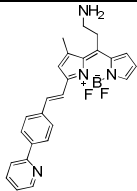
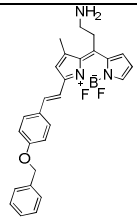
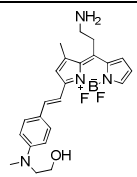
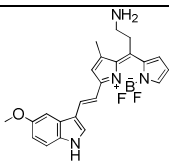
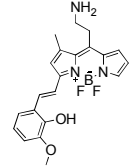
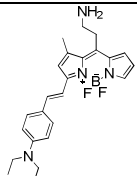
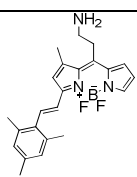
<b>BDM-7</b>		487.3	467.9	4.68	89%	566	591	0.37	6.6
<b>BDM-8</b>		417.3	418.0	2.31	95%	561	575	0.34	3.9
<b>BDM-9</b>		365.3	346.0	4.21	88%	554	567	0.33	3.5
<b>BDM-12</b>		385.3	365.9	4.46	90%	556	567	0.32	6.2
<b>BDM-14</b>		518.3	498.9	6.18	96%	593	624	0.02	7.8
<b>BDM-16</b>		485.4	466.0	5.46	94%	561	574	0.14	4.9
<b>BDM-18</b>		397.3	378.0	4.61	100%	567	588	0.33	6.7

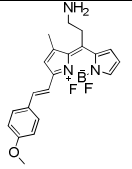
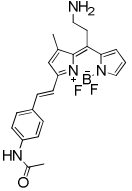
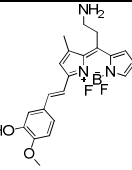
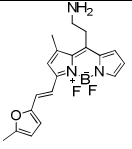
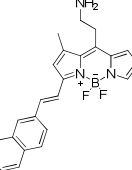
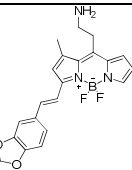
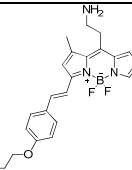
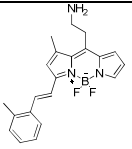
<b>BDM-19</b>		393.3	374.0	4.91	90%	555	569	0.71	8.0
<b>BDM-22</b>		341.3	322.0	3.61	85%	567	584	0.14	5.8
<b>BDM-30</b>		439.3	419.9	4.99	86%	596	634	0.11	4.4
<b>BDM-32</b>		431.3	412.0	4.62	91%	576	624	0.25	5.6
<b>BDM-33</b>		381.3	362.0	3.69	88%	564	580	0.14	9.7
<b>BDM-34</b>		415.3	396.0	4.98	92%	547	581	0.65	7.4
<b>BDM-36</b>		415.3	396.0	5.02	94%	568	595	0.23	6.9
<b>BDM-38</b>		432.3	411.9	3.71	87%	565	579	0.06	9.8

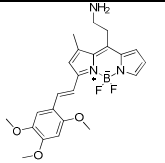
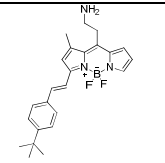
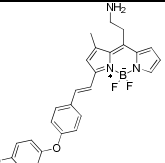
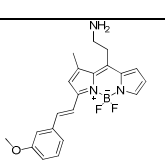
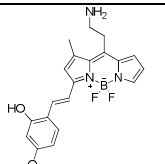
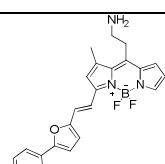
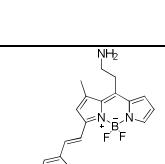
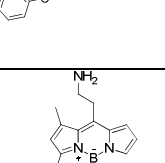
<b>BDM-40</b>		427.3	408.0	4.94	88%	554	567	0.53	5.6
<b>BDM-42</b>		473.3	454.0	5.06	93%	554	563	0.25	4.3
<b>BDM-43</b>		423.3	404.0	4.55	97%	564	579	0.21	4.5
<b>BDM-45</b>		451.3	432.0	5.47	93%	564	583	0.74	4.5
<b>BDM-46</b>		423.3	404.0	5.30	94%	564	583	0.53	6.0
<b>BDM-48</b>		407.3	388.0	4.46	98%	563	583	0.83	4.0
<b>BDM-49</b>		379.2	360.0	3.76	92%	562	572	0.24	5.7

<b>BDM-53</b>		439.3	420.0	4.07	87%	568	600	0.46	5.9
<b>BDM-54</b>		460.3	439.9 441.9	4.39	88%	559	573	0.52	6.2
<b>BDM-61</b>		431.3	411.9	4.73	91%	576	610	0.22	8.7
<b>BDM-62</b>		411.3	392.0	3.58	89%	567	594	0.43	5.2
<b>BDM-63</b>		425.3	406.0	4.01	94%	568	597	0.54	6.5
<b>BDM-65</b>		433.3	413.9	5.21	84%	589	615	0.15	7.2
<b>BDM-68</b>		435.3	415.9	4.90	87%	551	561	0.63	5.5

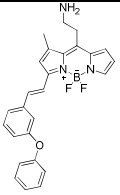
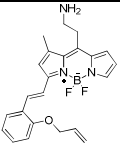
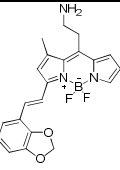
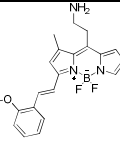
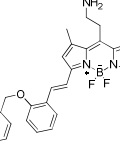
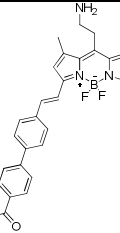
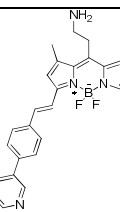
<b>BDM-69</b>		453.3	434.2	5.01	94%	574	594	0.32	8.6
<b>BDM-70</b>		461.3	442.0	4.82	93%	582	642	0.13	7.1
<b>BDM-73</b>		446.3	425.8 427.8	3.89	84%	561	575	0.28	4.4
<b>BDM-75</b>		423.3	404.0	4.64	88%	560	585	0.53	4.4
<b>BDM-76</b>		439.3	420.0	5.20	84%	572	588	0.25	4.0
<b>BDM-77</b>		393.3	374.0	5.03	84%	557	569	0.54	5.2
<b>BDM-78</b>		439.3	420.0	4.55	87%	591	n.d	0.01	5.0

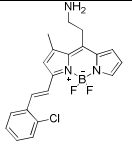
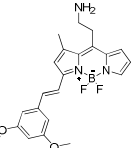
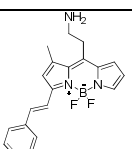
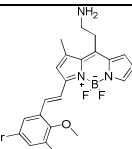
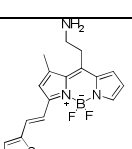
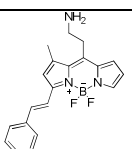
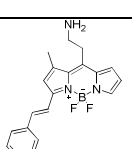
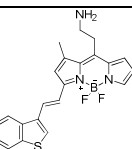
<b>BDM-88</b>		428.3	409.0 429.0	3.57	95%	565	576	0.21	4.9
<b>BDM-90</b>		457.3	438.0	5.18	97%	565	582	0.26	7.3
<b>BDM-91</b>		424.3	405.0	3.59	95%	614	699	0.02	7.0
<b>BDM-93</b>		420.3	401.0	3.95	91%	592	653	0.06	4.0
<b>BDM-97</b>		397.3	378.0	3.68	89%	561	572	0.04	6.8
<b>BDM-107</b>		422.3	403.0	4.22	97%	617	681	0.05	4.7
<b>BDM-108</b>		393.3	374.1	4.86	85%	549	573	0.35	6.2

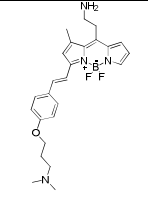
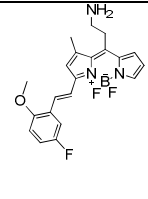
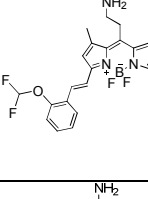
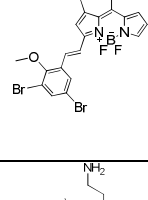
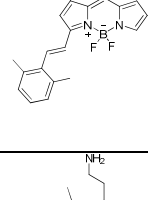
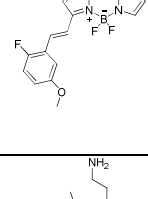
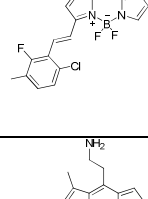
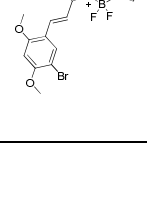
<b>BDM-110</b>		381.3	362.0	4.11	91%	563	583	0.85	3.5
<b>BDM-111</b>		408.3	389.0	3.11	100%	566	589	0.79	4.7
<b>BDM-132</b>		397.3	378.0	3.36	100%	568	594	0.05	4.5
<b>BDM-135</b>		355.3	336.0	3.98	93%	577	601	0.10	4.4
<b>BDM-137</b>		401.3	382.0	4.84	87%	563	575	0.28	7.1
<b>BDM-139</b>		395.2	376.0	3.94	92%	564	584	0.55	3.7
<b>BDM-140</b>		409.3	390.0	4.97	93%	564	585	0.57	5.6
<b>BDM-143</b>		365.2	346.0	4.51	84%	554	566	0.42	6.1

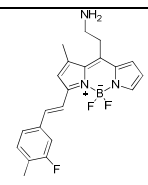
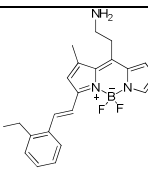
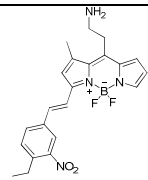
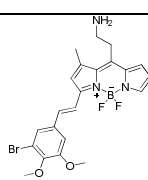
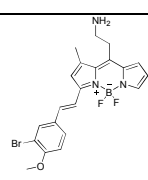
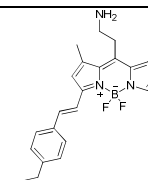
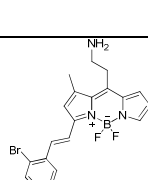
<b>BDM-144</b>		441.3	422.0	3.67	94%	578	612	0.05	5.4
<b>BDM-177</b>		407.3	388.0	5.03	96%	556	567	0.78	4.1
<b>BDM-178</b>		473.2	454.0	5.06	96%	561	577	0.37	5.0
<b>BDM-186</b>		381.2	362.0	4.15	97%	553	564	0.97	5.4
<b>BDM-192</b>		397.2	378.0	3.75	86%	574	605	0.20	4.0
<b>BDM-195</b>		481.7	461.9	5.18	100%	600	663	0.03	6.5
<b>BDM-101</b>		443.3	423.9	5.23	97%	559	576	0.66	5.3
<b>BDM-100</b>		436.1	415.8 417.8	4.49	86%	571	582	0.43	5.0

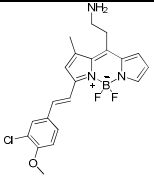
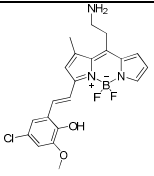
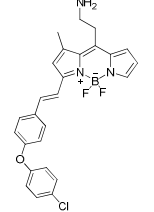
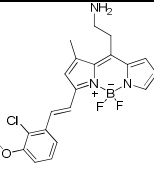
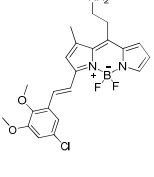
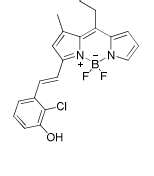
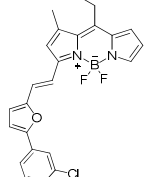


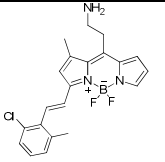
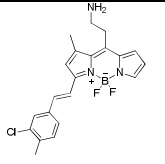
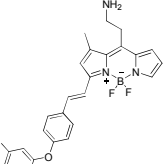
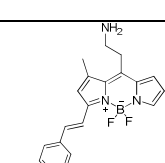
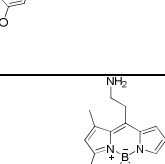
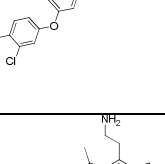
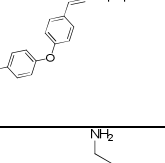
<b>BDM-20</b>		443.3	424.0	5.09	94%	554	564	0.47	4.4
<b>BDM-202</b>		407.3	388.0	4.64	85%	559	575	0.52	4.1
<b>BDM-231</b>		395.2	376.0	3.94	93%	558	568	0.17	5.9
<b>BDM-198</b>		381.2	362.0	4.08	95%	559	574	0.59	5.2
<b>BDM-218</b>		457.3	438.0	5.18	100%	559	574	0.37	5.8
<b>BDM-179</b>		485.3	466.0	5.09	96%	566	581	0.26	5.5
<b>BDM-199</b>		429.3	410.0	3.79	94%	562	574	0.18	7.6

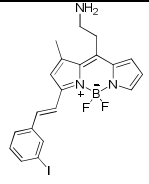
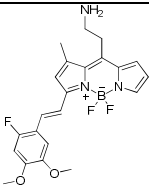
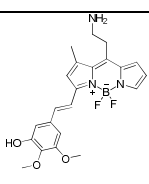
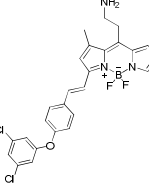
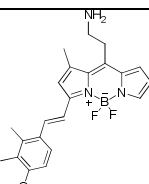
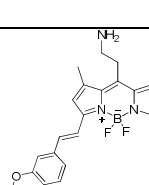
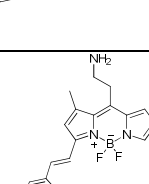
<b>BDM-207</b>		385.7	366.0	4.47	88%	553	566	0.24	3.9
<b>BDM-209</b>		411.3	392.0	4.09	93%	555	567	0.38	4.1
<b>BDM-237</b>		477.1	457.8	4.69	97%	558	572	0.35	5.2
<b>BDM-228</b>		490.2	469.8 471.9	4.48	92%	557	567	0.24	8.8
<b>BDM-236</b>		371.3	352.0	4.29	90%	574	594	0.22	4.9
<b>BDM-208</b>		365.2	346.1	4.54	100%	558	572	0.27	3.8
<b>BDM-27</b>		351.2	332.0	4.01	87%	553	566	0.39	4.2
<b>BDM-37</b>		407.3	387.9	4.81	84%	566	588	0.15	4.5

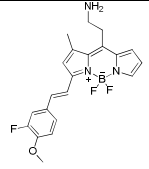
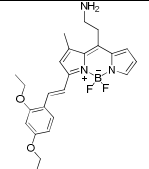
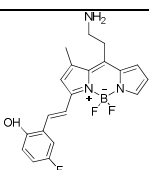
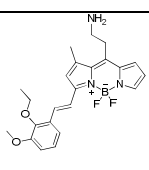
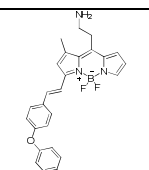
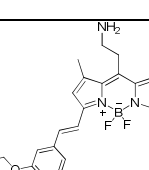
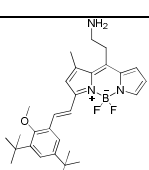
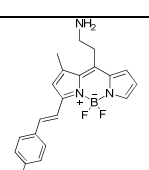
<b>BDM-163</b>		452.4	453.0	2.78	88%	566	586	0.41	5.6
<b>BDM-239</b>		399.2	380.0	4.42	100%	559	572	0.28	5.5
<b>BDM-240</b>		417.2	397.9	4.48	87%	552	565	0.23	5.5
<b>BDM-241</b>		539.0	517.8	4.88	84%	560	576	0.32	6.5
<b>BDM-243</b>		379.3	360.0	4.72	89%	543	565	0.87	3.0
<b>BDM-245</b>		399.2	380.0	4.32	87%	555	563	0.32	4.4
<b>BDM-246</b>		417.7	397.9	4.93	100%	554	566	0.17	5.8
<b>BDM-247</b>		490.2	469.9	4.48	90%	571	599	0.54	5.6
			471.9	4.67					

<b>BDM-249</b>		383.2	364.0	4.72	100%	557	568	0.24	4.8
<b>BDM-251</b>		379.3	360.0	4.84	100%	556	572	0.22	5.9
<b>BDM-252</b>		424.3	405.0	4.86	91%	556	569	0.08	4.6
<b>BDM-259</b>		490.2	469.8 471.8	4.70	87%	559	573	0.35	5.0
<b>BDM-260</b>		460.1	439.8 441.8	4.55	93%	564	582	0.05	4.0
<b>BDM-263</b>		407.3	388.0	5.69	85%	559	571	0.26	3.9
<b>BDM-267</b>		444.1	423.9 425.9	4.96	92%	558	573	0.21	4.4

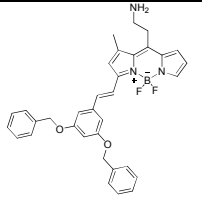
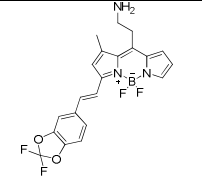
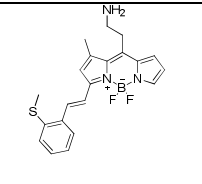
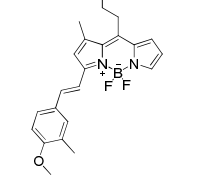
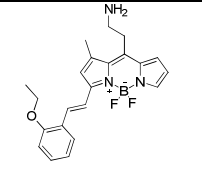
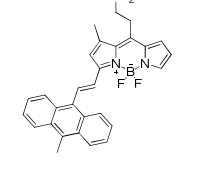
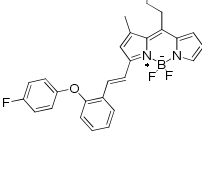
<b>BDM-274</b>		415.7	395.9	4.48	93%	562	577	0.46	3.9
<b>BDM-275</b>		431.7	411.9	4.30	85%	562	n.d	0.05	5.9
<b>BDM-277</b>		477.7	457.9	5.71	87%	559	574	0.59	4.9
<b>BDM-281</b>		415.7	395.9	4.13	92%	554	567	0.28	5.1
<b>BDM-282</b>		445.7	425.9	4.74	88%	558	565	0.19	4.5
<b>BDM-283</b>		401.7	381.9	3.68	100%	556	567	0.15	4.3
<b>BDM-284</b>		451.7	431.9	5.23	84%	594	622	0.03	4.6

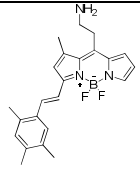
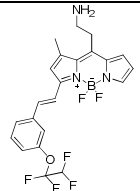
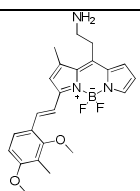
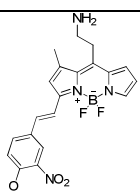
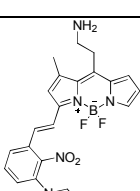
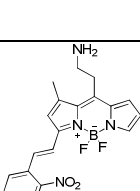
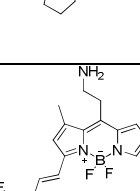
<b>BDM-285</b>		399.7	379.9	4.74	86%	544	561	0.51	6.0
<b>BDM-289</b>		399.7	380.0	4.97	84%	559	570	0.26	4.9
<b>BDM-290</b>		477.7	457.9	5.61	85%	558	574	0.36	4.5
<b>BDM-298</b>		473.3	454.0	5.30	89%	559	568	0.32	6.8
<b>BDM-299</b>		512.2	491.8 493.8	5.89	91%	555	563	0.27	7.1
<b>BDM-300</b>		457.3	438.0	5.65	89%	562	579	0.44	5.3
<b>BDM-301</b>		461.3	442.0	4.76	100%	563	586	0.41	5.6

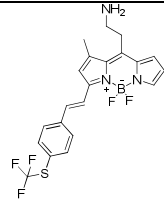
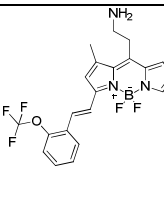
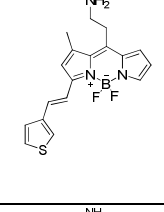
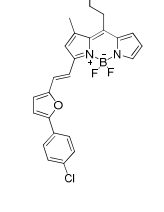
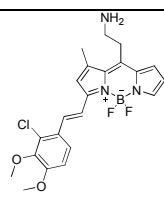
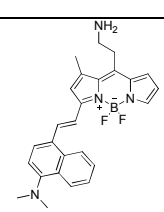
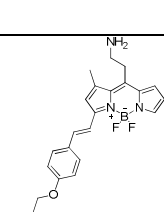
<b>BDM-303</b>		477.1	457.8	4.92	100%	555	566	0.31	5.6
<b>BDM-305</b>		429.2	410.0	3.99	86%	567	587	0.25	8.1
<b>BDM-307</b>		427.3	408.0	3.50	84%	564	580	0.07	4.0
<b>BDM-308</b>		512.2	491.8	6.15	86%	556	567	0.19	4.9
<b>BDM-310</b>		409.3	390.0	4.90	84%	566	600	0.42	6.5
<b>BDM-311</b>		461.3	441.9	5.28	84%	556	565	0.21	5.1
<b>BDM-312</b>		399.2	380.0	4.36	83%	557	568	0.18	3.0

<b>BDM-314</b>		399.2	380.0	4.26	100%	556	570	0.10	4.7
<b>BDM-316</b>		439.3	420.0	4.81	87%, 4.81	572	610	0.46	5.9
<b>BDM-318</b>		385.2	366.0	3.83	85%, 3.83	563	576	0.11	7.4
<b>BDM-320</b>		425.3	406.0	4.46	84%	558	569	0.21	4.3
<b>BDM-322</b>		461.3	441.9	5.37	85%	559	577	0.15	5.5
<b>BDM-323</b>		395.3	376.0	4.61	87%	556	570	0.44	5.0
<b>BDM-325</b>		493.4	474.0	6.59	85%	557	573	0.47	5.3
<b>BDM-326</b>		417.2	398.0	4.40	91%	554	565	0.71	5.9

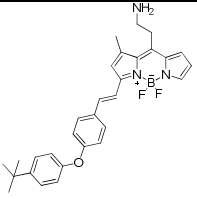
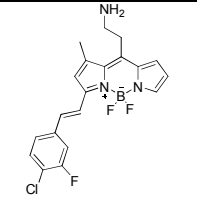
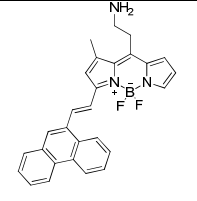
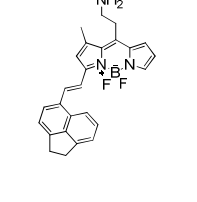
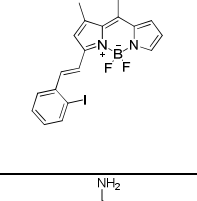
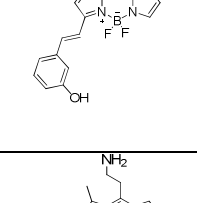
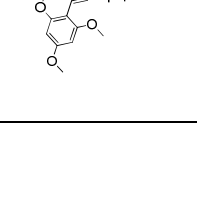


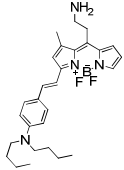
<b>BDM-331</b>		563.4	543.9	6.05	84%	554	566	0.65	9.3
<b>BDM-332</b>		431.2	411.9	4.83	91%	552	562	0.61	5.3
<b>BDM-333</b>		397.3	378.0	4.51	95%	557	575	0.30	5.6
<b>BDM-335</b>		395.3	376.0	4.57	95%	565	591	0.78	6.2
<b>BDM-336</b>		395.3	376.0	4.53	91%	560	577	0.58	3.4
<b>BDM-340</b>		465.3	445.9	5.43	96%	534	541	0.11	5.0
<b>BDM-341</b>		461.3	441.9	5.09	90%	556	570	0.37	12.4

<b>BDM-343</b>		393.3	374.0	5.08	91%	559	577	0.28	9.6
<b>BDM-345</b>		467.2	447.9	4.92	88%	551	564	0.22	7.4
<b>BDM-347</b>		425.3	406.0	4.67	96%	566	591	0.57	5.3
<b>BDM-350</b>		426.2	406.9	3.93	98%	556	571	0.14	5.9
<b>BDM-356</b>		479.3	460.0	5.16	92%	573	682	0.03	4.2
<b>BDM-357</b>		465.3	446.0	4.72	90%	585	687	0.04	5.0
<b>BDM-359</b>		399.2	380.0	4.33	100%	559	574	0.83	6.6

<b>BDM-363</b>		451.3	431.8	4.98	96%	553	564	0.51	6.1
<b>BDM-365</b>		435.2	415.9	4.77	96%	549	563	0.24	5.2
<b>BDM-369</b>		357.2	337.9	3.96	93%	554	570	0.30	3.6
<b>BDM-371</b>		451.7	431.9	5.35	90%	590	630	0.03	4.8
<b>BDM-372</b>		445.7	425.9	4.34	87%	561	578	0.55	8.5
<b>BDM-377</b>		444.3	445.0	4.76	98%	586	n.d	0.04	6.9
<b>BDM-378</b>		475.3	456.0	5.14	94%	563	585	0.41	3.8

<b>BDM-391</b>		379.2	360.0	3.86	91%	554	563	0.31	5.3
<b>BDM-397</b>		411.2	392.0	3.67	92%	570	614	0.10	4.9
<b>BDM-401</b>		469.3	449.9	4.28	100%	565	590	0.85	5.6
<b>BDM-409</b>		430.1	409.9 411.8	4.93	85%	558	570	0.12	4.0
<b>BDM-425</b>		445.3	425.9	5.27	89%	562	576	0.12	4.4
<b>BDM-429</b>		395.3	376.0	4.49	100%	564	586	0.23	4.6
<b>BDM-430</b>		383.3	364.0	3.09	100%	565	592	0.99	3.3

<b>BDM-435</b>		499.4	480.0	6.14	94%	555	565	0.39	4.9
<b>BDM-437</b>		403.6	383.9	4.62	95%	555	566	0.21	4.1
<b>BDM-440</b>		451.3	432.0	5.42	93%	563	589	0.37	6.1
<b>BDM-89</b>		427.3	408.0	5.15	85%	576	612	0.30	6.1
<b>BDM-384</b>		477.1	457.8	4.60	92%	551	565	0.32	3.1
<b>BDM-105</b>		367.2	348.0	3.48	93%	556	567	0.18	4.4
<b>BDM-82</b>		441.3	422.0	4.36	87%	579	621	0.40	6.6

<b>BDM-17</b>		478.4	459.0 479.0	6.17	89%	622	695	0.03	4.0
---------------	---	-------	----------------	------	-----	-----	-----	------	-----

HPLC conditions: A: H<sub>2</sub>O-HCOOH: 99.9:0.1. B: ACN-HCOOH: 99.9:0.1; gradient 5% B to 95% B (10 min), isocratic 95% B (2 min). Reverse-phase Agilent C<sub>18</sub> Zorbax column (2.1 x 30 mm<sup>2</sup>) 3.5 μm, flow rate: 1 mL/min. Purity determined by integration of the absorbance peaks at 350 nm. ESI (+) *m/z* signals mostly correspond to the [M-F] fragmentation.

### 3. Characterization data for Ig Orange (BDM-69).

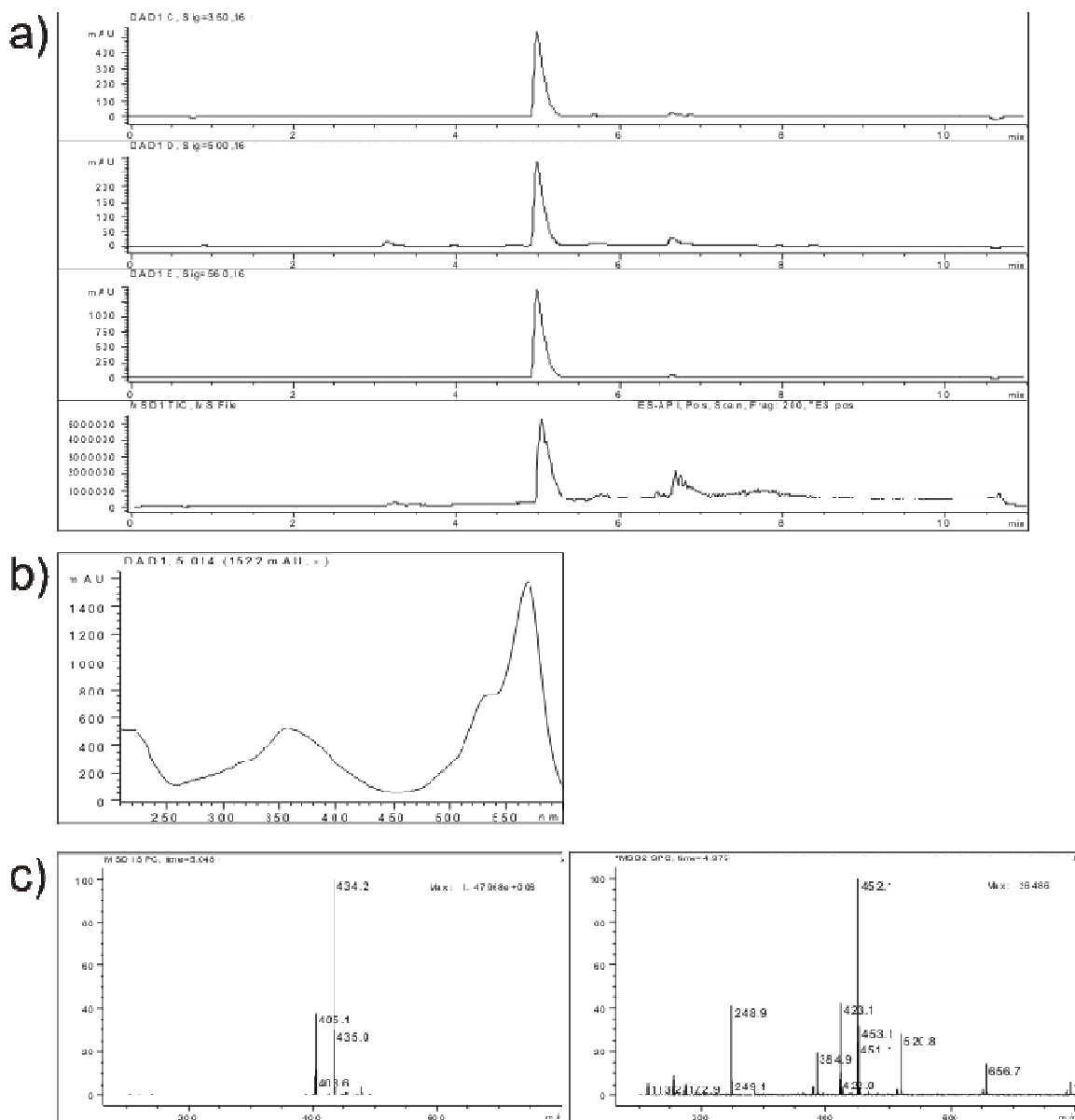


**Figure S1. HPLC-MS characterization of Ig Orange (BDM-69).** a) Chromatograms (*descending order*) at 350 nm, 500 nm, 560 nm and MS-TIC; b) absorbance spectra; c) *left, right*: ESI-positive and ESI-negative MS spectra, respectively.

#### **4. Extended screening of Ig Orange (BDM-69).**

Fluorescence intensities were measured using a Spectra Max Gemini XSF plate reader in a 384-well plate. **IgG orange** was dissolved to a final concentration of 10  $\mu\text{M}$  (20 mM HEPES buffer, pH 7.4, containing 1% DMSO) and incubated with different biomolecules at 4 serial concentrations (*see below*) in 20 mM HEPES buffer (pH 7.4). The excitation wavelength was set at 510 nm, and the emission spectra were recorded from 560 to 700 nm. Fluorescence increase ratios were determined by referring the fluorescence intensity emission (590 nm) of **Ig Orange** in the presence of the screened analytes to the fluorescence intensity emission of **Ig Orange** in the absence of the screened analytes.

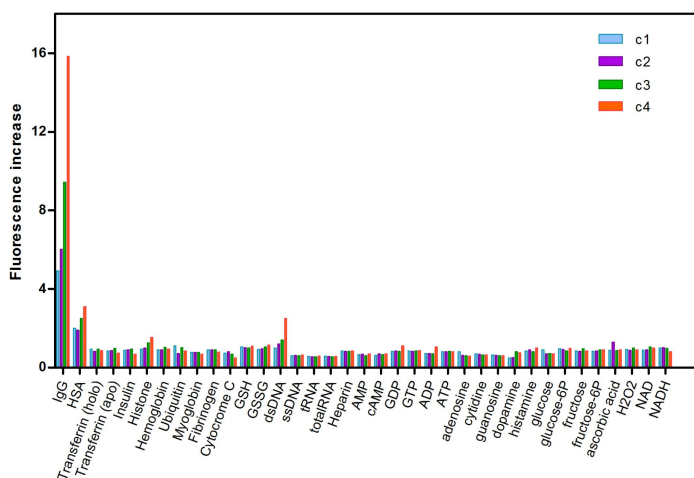


**Figure S2.** Fluorescence response of **Ig Orange** against an extended set of macromolecules and small molecules in 20 mM HEPES buffer, pH 7.4 (fold increase determined at 590 nm). Analyte serial concentrations (c1-c4, ascending concentration order): proteins, peptides, dsDNA, ssDNA, tRNA, total RNA and heparin: 0.125, 0.25, 0.5 and 1 mg/mL; AMP, cAMP, GDP, GTP, ADP, ATP, adenosine, cytidine, guanosine: 12.5, 25, 50, 100  $\mu\text{M}$ ; dopamine, histamine: 0.04, 0.2, 1 and 5 mg/mL; glucose, glucose-6P, fructose, fructose-6P: 0.08, 0.4, 2, 10 mM; ascorbic acid, H<sub>2</sub>O<sub>2</sub>, NAD, NADH: 0.04, 0.2, 1, 5 mM.



**IgG Orange** was dissolved to a final concentration of 10  $\mu\text{M}$  (PBS buffer, pH 7.3, containing 1% DMSO) and incubated with human IgG, IgA and IgM at different concentrations (*see below*) in PBS buffer (pH 7.3). The excitation wavelength was set at 530 nm, and fluorescence fold increase ratios were determined by referring the maximum fluorescence intensity emission (590 nm) of **Ig Orange** in the presence of immunoglobulins to the maximum fluorescence intensity emission of **Ig Orange** in buffer.

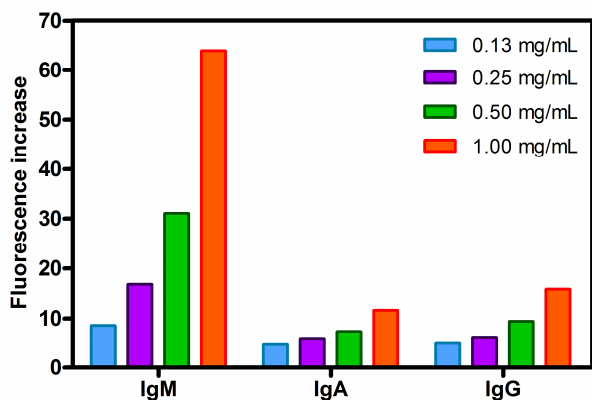


**Figure S3.** Fluorescence response of **IgG orange** upon incubation with different concentrations of human IgM, IgA and IgG.

### **5. Ig Orange response against IgG in human serum samples.**

Known amounts of human IgG covering the whole physiological range (3.3, 6.2, 9.4 and 12.5 mg/mL) were added to immunoglobulin(G, A, M)-depleted human serum (Sigma Aldrich). The resulting samples were diluted 10 times in PBS buffer (pH 7.3) to reach a final volume of 100  $\mu$ L and **Ig Orange** (1  $\mu$ L, 1 mM) was added (final **Ig Orange** concentration: 10  $\mu$ M). Fluorescence intensities of the samples were recorded on a SpectraMax M2 plate reader (exc: 530 nm; emission: 590 nm). The experimental data was fitted to a linear regression using Graphpad Prism 5.0 software.

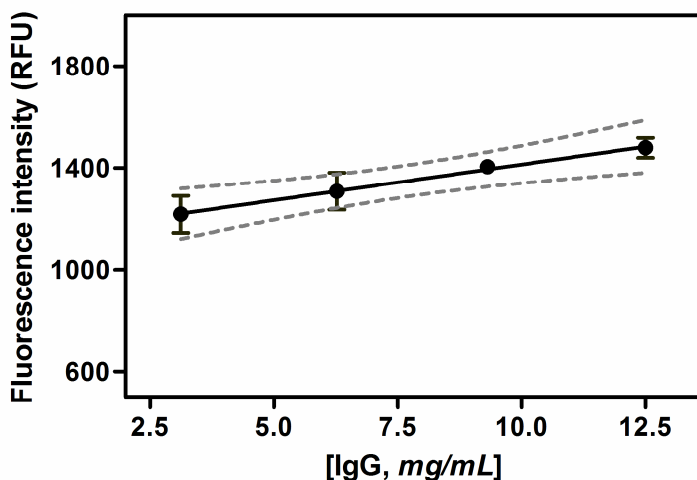


**Figure S4.** Fluorescence response of **Ig Orange** against known concentrations of IgG in immunoglobulin-depleted human serum. Values are represented as means ( $n=3$ ) and errors bars as standard deviations. Dotted grey lines indicate a 95% reliability interval. Regression coefficient ( $R^2$ ): 0.99.

## 6. Characterization of biotinylated human IgG.

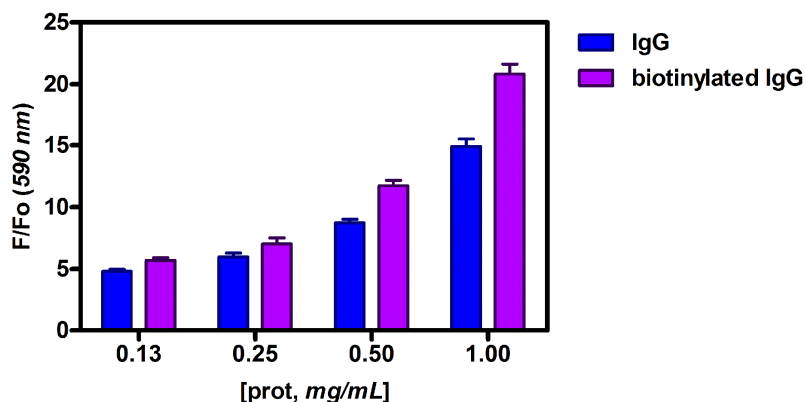


**Figure S5.** Comparative fluorescence increase of **Ig Orange** after incubation with different concentrations of non-modified and biotinylated human IgG. Values are represented as means ( $n=3$ ) and error bars as standard deviations.

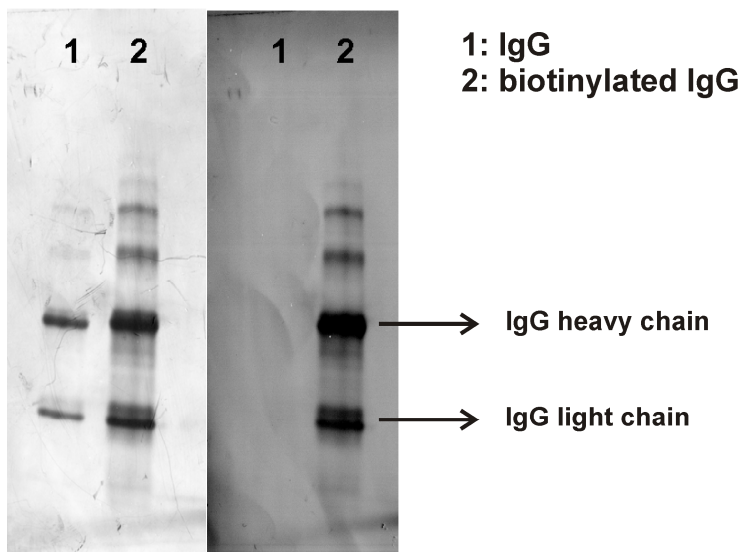


**Figure S6.** SDS-PAGE gel and Western blotting of human non-modified and biotinylated IgG. *Left*) samples were solved by SDS-PAGE and stained with Coomassie Blue; *right*) samples were solved by Western blotting and immunoblots were incubated with HRP-conjugated streptavidin.

## 7. Structure-fluorescence relationships of Ig Orange and additional SPR experiments.

**Ig Orange (BDM-69)** (10  $\mu\text{M}$ ) and **BD-69** (10  $\mu\text{M}$ ) (previously synthesized as in ref. 20 in the manuscript) were incubated with different concentrations of human IgG in 20 mM HEPES buffer (pH 7.4) and the fluorescence intensities were recorded on a SpectraMax M2 plate reader (excitation: 530 nm; emission: 590 nm). Values are represented as means ( $n=3$ ) of the fluorescence fold increase after incubation with the protein.

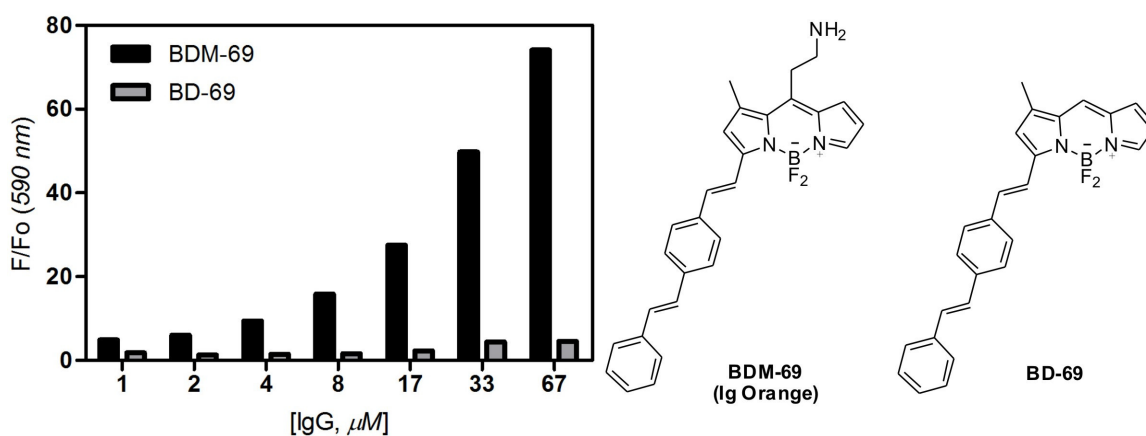


**Figure S7.** Fluorescence response of **Ig Orange (BDM-69)** and **BD-69** vs. human IgG. A 15-fold higher fluorescence increase was observed in the case of **Ig Orange** indicating the relevant contribution of the aminoethyl group in the interaction with human IgG.

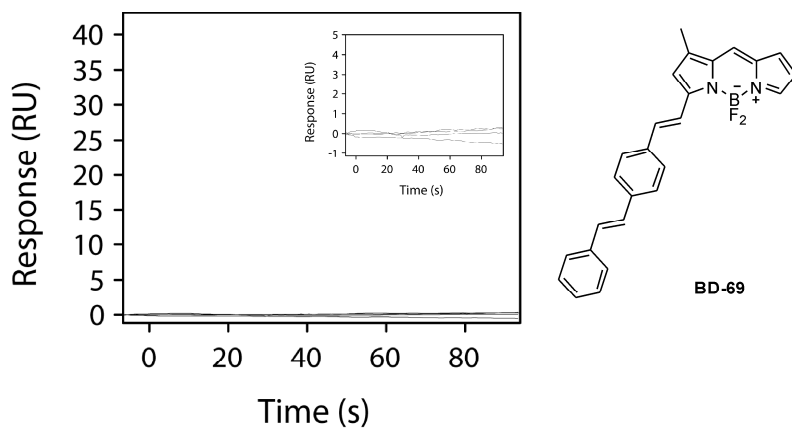


**Figure S8.** Binding sensorgrams of the aminoethyl-free compound (**BD-69**) upon injection across an immobilized immunoglobulin chip. Different concentrations of **BD-69** were injected across a control surface and the immobilized surface serially as described in the Experimental Section for **Ig Orange**. *Inset*) zoom image of the sensorgrams.

### **8. Binding of Ig Orange to polyclonal IgG and monoclonal IgG<sub>1</sub>.**

**Ig Orange** (10  $\mu$ M) was incubated with different concentrations of IgG from human serum (polyclonal IgG) and a monoclonal human IgG<sub>1</sub> in 20 mM HEPES buffer (pH 7.4). Fluorescence measurements were recorded on a SpectraMax M2 plate reader (excitation: 530 nm; emission: 590 nm).

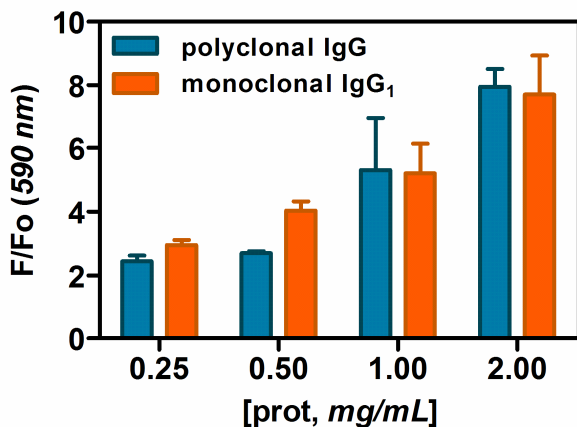


**Figure S9.** Fluorescence intensities of **Ig Orange** after incubation with polyclonal human IgG and monoclonal human IgG<sub>1</sub>. Values are represented as means ( $n=3$ ) and error bars as standard deviations.

### **9. Fractional saturation curve experiments of Ig Orange.**

**Ig Orange** (10  $\mu\text{M}$ ) was incubated with different concentrations of human IgG in 20 mM HEPES buffer (pH 7.4) and the fluorescence intensities were recorded on a SpectraMax M2 plate reader (excitation: 530 nm; emission: 590 nm).

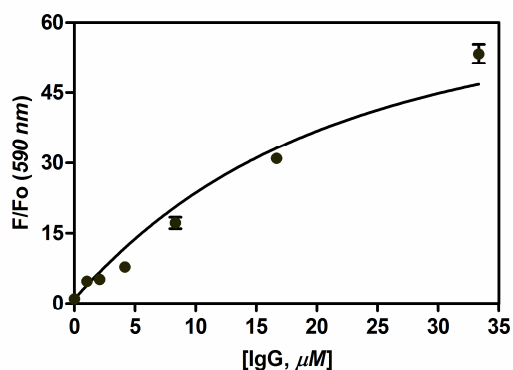


**Figure S10.** Fluorescence-based fractional saturation curve of **Ig Orange**. Values were represented as means ( $n=3$ ) of the fluorescence fold increase after incubation with the protein, and adjusted to a binding saturation curve (GraphPad Prism 5.0) to estimate a dissociation constant  $K_D$ :  $14.1 \pm 0.9 \mu\text{M}$ .

## **References**

1. A. Nierth, A. Y. Kobitski, G. U. Nienhaus and A. Jaschke, *J. Am. Chem. Soc.* 2010, **132**, 2646.
2. S. A. Fieldhouse and I. R. Peat, *J. Phys. Chem.* 1969, **73**, 275.
3. S. Rishikesan, S. Gayen, Y. R. Thaker, S. Vivekanandan, M. S. Manimekalai, Y. H. Yau, S. G. Shochat and G. Gruber, *Biochim. Biophys. Acta* 2009, **1787**, 242.
4. D. G. Myszka, *J. Mol. Recognit.* 1999, **12**, 279.